Contact Area Lithography (CAL): A New Approach to Direct Formation of Nanometric Chemical Patterns

Changdeuck Bae and Hyunjung Shin*

School of Advanced Materials Engineering, Kookmin University, Seoul 136-702, Korea

Jooho Moon

School of Advanced Materials Engineering, Yonsei University, Seoul 120-749, Korea

Myung M. Sung

Department of Chemistry, Kookmin University, Seoul 136-702, Korea

Received September 16, 2005
Revised Manuscript Received January 2, 2006

Nanometric chemical patterns have received increasing attention because of their chemical contrast, biologically relevant size, and high areal density. Immobilized biomolecules on such chemical patterns not only provide us with an integrated understanding of biomolecular functions in biological systems[1,2] but are also important for highly sensitive detection with minimal sample consumption in medical diagnostics.[3,4] Very recently, chemical patterns with dimensions below 100 nm have been reported for biological applications.[3−7] A procedure based on scanning probe achieves arrays of biomolecules with well-defined feature sizes below 100 nm and controlled position,[3,5,7] but the writing speed under these methods are presumably quite low. Another candidate, which does not have this shortcoming, is the method that uses monodispersed spherical colloids.[8] Since the introduction of the feasibility of lithography by utilizing colloidal particles by Deckman et al.,[9] the group of Van Duyne has extended the lithography with 2D close-packed particles and named it nanosphere lithography (NSL).[10] In NSL, the ordered arrays of interstices between the assembled particles are used as a site of either material deposition or ion/plasma etching forming the periodic arrays of topographic structures.[10,11] However, NSL additionally requires a surface modification step such as the formation of self-assembled monolayers (SAMs) onto the physical patterns to render chemical contrasts on them. Here we describe a novel (see two other contributions),[12,13] direct method, termed contact area lithography (CAL), that directly generates periodic surface chemical patterns (PSCPs) at the sub-100 nm scale. In addition, we demonstrate that this strategy makes possible both the fabrication of isolated TiO_2 nanodisc arrays and the fabrication of SiO_2 nanocavity arrays using PSCPs on octadecyltrichlorosilane (OTS) SAMs. That is, a selective atomic layer deposition (ALD) as well as a selective chemical etching process can be applied to the PSCPs produced by CAL, where the patterned SAM layer functions as superior chemical patterns. Finally, we propose a simple equation to estimate the sizes of resulting patterns from such lithography and discuss the role of the capillary meniscus on the determination of pattern size.

The patterning began by dispersing monodisperse silica particles of 200−500 nm in diameter prepared by the Stöber et al. method[14] in aqueous solutions. A droplet of the suspension was placed on the center of a cylindrical drying cell, which is glued to the substrate, by using a micropipet. In the drying cell, the suspension was geometrically confined for the drying-mediated self-assembly.[15] The quantity of dropped silica particles, which is the 5 μL dispersion with typical concentration of 0.5 wt % of the particles, was calculated to cover the area of the drying cell with a monolayer of particles. In the cell, the dropped dispersion was wetted on the surface of the substrate, resulting in a meniscus of slightly concave shape. As the solvent evaporated, nucleation of the silica particles started near the three-phase-contact line at the center of the cell. Subsequently, crystal growth propagated outward by lateral capillary forces between the particles. At the same time, the particles moved toward the contact line by convective transport flow, as had previously been reported by other researchers.[16] Following such a series of self-ordering processes, well-ordered two-dimensional (2D) arrays with polydomains were formed, and each domain was of an area of a few hundred square micrometers (Figure 1a).

Next, the substrate with the 2D colloidal crystals was plunged into a vessel of anhydrous toluene solutions containing OTS molecules, and the molecules formed SAMs on the entire area of the hydroxyl surfaces except those contacted by the crystals (Figure 1b). Note that the colloidal assembly

* Corresponding author. E-mail: hjshin@kookmin.ac.kr.

(1) Brower, V. *EMBO Rep.* **2001**, *2*, 558.
(2) MacBeath, G. *Nat. Genet.* **2002**, *32* (Suppl.), 526.
(3) Lee, K.-B.; Kim, E.-Y.; Mirkin, C. A.; Wolinsky, S. M. *Nano Lett.* **2004**, *4*, 1869.
(4) Vörös, J.; Blatter, T.; Textor, M. *MRS Bull.* **2005**, *30*, 202.
(5) Lee, K.-B.; Park, S.-J.; Mirkin, C. A.; Smith, J. C.; Mrksich, M. *Science* **2002**, *295*, 1702.
(6) Michel, R.; Reviakine, I.; Sutherland, D.; Fokas, C.; Csucs, G.; Danuser, G.; Spencer, N. D.; Textor, M. *Langmuir* **2002**, *18*, 8580.
(7) Gu, J.; Yam, C. M.; Li, S.; Cai, C. *J. Am. Chem. Soc.* **2004**, *126*, 8098.
(8) Valsesia, A.; Colpo, P.; Silvan, M. M.; Meziani, T.; Ceccone, G.; Rossi, F. *Nano Lett.* **2004**, *4*, 1047.
(9) (a) Deckman, H. W.; Dunsmuir, J. H. *Appl. Phys. Lett.* **1982**, *41*, 377. (b) Deckman, H. W.; Dunsmuir, J. H. *J. Vac. Sci. Technol.* **1983**, *B1*, 1109.
(10) (a) Hulteen, J. C.; Van Duyne, R. P. *J. Vac. Sci. Technol.* **1995**, *A13*, 1553. (b) Haynes, C. L.; Van Duyne, R. P. *J. Phys. Chem. B* **2001**, *105*, 5599.
(11) Whitney, A. V.; Myers, B. D.; Van Duyne, R. P. *Nano Lett.* **2004**, *4*, 1507.
(12) Cai, Y.; Ocko, B. M. *Langmuir* **2005**, *21*, 9274.
(13) McLellan, J. M.; Geissler, M.; Xia, Y. *Chem. Phys. Lett.* **2005**, *408*, 80.
(14) Stöber, W.; Berner, A.; Blaschke, R. *J. Colloid Interface Sci.* **1969**, *29*, 710.
(15) Denkov, N.; Velev, O.; Kralchevsky, P.; Ivanov, I.; Yoshimura, H.; Nagayama, K. *Langmuir* **1992**, *8*, 3183.
(16) (a) Dimitrov, A.; Nagayama, K. *Langmuir* **1996**, *12*, 1303. (b) Kralchevsky, P.; Nagayama, K. *Langmuir* **1994**, *10*, 23. (c) Tessier, P.; Velev, O.; Kalambur, A.; Lenhoff, A.; Rabolt, J.; Kaler, E. *Adv. Mater.* **2001**, *13*, 396.

10.1021/cm052084m CCC: $33.50
Published on Web 02/07/2006

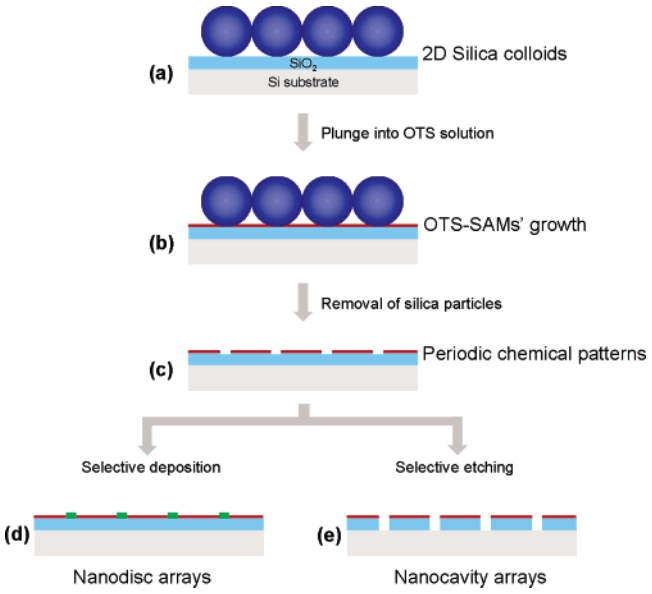

Figure 1. Schematic illustration of the CAL procedure. (a) 2D crystallization of colloidal spheres on the substrates. (b) Coating the SAMs of OTS molecules. (c) Removal of the crystallized particles. (d) Selective deposition by ALD. (e) Selective wet etching by chemical etchant.

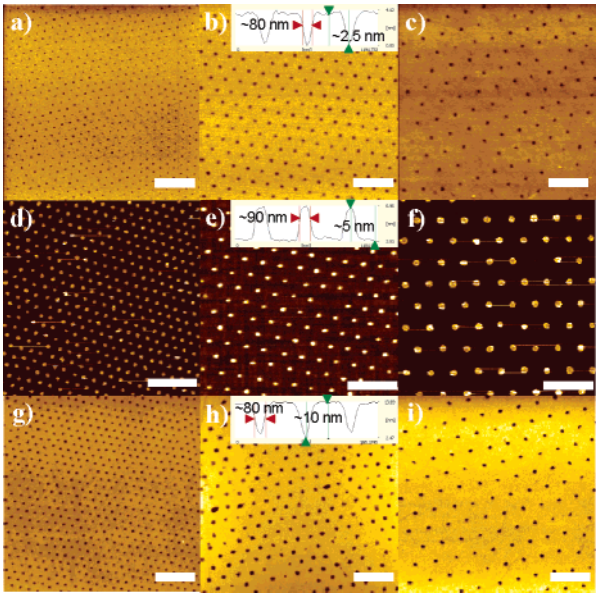

Figure 2. Series of AFM topographical images. (a−c) Resulting patterns in OTS SAMs of 52 ± 4, 79 ± 7, and 94 ± 5 nm in diameter, respectively, formed by different sizes of the colloidal particles (200, 350, and 500 nm in diameter). (d−f) TiO_2 nanodiscs fabricated by ALD of 66 ± 7, 85 ± 16, and 128 ± 13 nm in diameter, respectively, using the PSPCs in OTS−SAMs as shown in parts a−c. (g−i) SiO_2 nanocavities fabricated by chemical wet etching of 64 ± 8, 96 ± 9, and 100 ± 14 nm in diameter, respectively, using the PSPCs in OTS SAMs as shown in parts a−c. The insets show the AFM line-profile images of the nanostructures fabricated by CAL using 350 nm silica colloids. The red arrows indicate the widths of the nanostructures, and the green arrows show the heights of the structures. All scale bars correspond to 1 μm.

was not disassembled at all but intact during the immersion. The structural integrity of the 2D colloidal crystals could be explained by two different types of bridges. One is a liquid bridge, a so-called "capillary bridge," which contributes to strong cohesive capillary forces.[17] This is developed by the confined liquids at the particle−substrate and particle−particle contacts. The other one is a solid bridge, which is formed by reprecipitation of species dissolved from the oxide surfaces of the colloids. Although the solid bridge is as small as a few nanometers depending on the degree of oxidation, it can induce a far stronger interparticle bond than the former.[18]

Several hours later, the OTS grown substrate was taken out of the solutions and was immersed in pure water to terminate the reaction of active headgroup of remaining OTS molecules, preventing them from being redeposited onto the opened holes in OTS−SAMs after removal of the assembled particles. The removal of attached particles was conducted by sonication in an aqueous medium, and the substrate was dried with a stream of nitrogen gas (Figure 1c). Well-defined PSCPs in OTS−SAMs with hexagonal geometry were observed by a contact-mode atomic force microscopy (AFM) as shown in Figure 2a−c. The diameters of the resulting holes were 52 ± 4, 79 ± 7, and 94 ± 5 nm in the cases of using particles of about 200, 350, and 500 nm in diameter, respectively. No defects were observed in Figure 2b, and only several point defects were detected in Figure 2a,c, whereas in the case of the larger area scan with 10 × 10 μm (not shown here), very few defects, which were mostly domain boundaries owing to the stacking faults during colloidal assembly, were observed. The average depth of the patterned holes in OTS SAMs was ∼2.51 nm (see inset in Figure 2b), which is in excellent agreement with the thickness of a fully grown OTS SAM layer.[19] The interhole spacing readily corresponded to the diameters of the silica particles measured by dynamic light scattering, which suggests an areal density or spacing could, in principle, be controlled by using the desired sizes of colloids.

Upon creation of PSCPs with CAL, a variety of surface nanostructures were successfully fabricated by chemical means. First, regular arrays of isolated nanodiscs of TiO_2 were fabricated by the selective deposition using ALD (Figure 1d). As an OTS molecule has an inert methyl group in its tail, which is resistant to deposition of materials during the processes of ALD coating, deposition of TiO_2 only took place onto the opened areas, that is, no coatings of OTS SAMs, of the substrate. Figure 2d−f shows the nanodisc arrays of TiO_2 with various areal densities, whereas there is no deposition of TiO_2 on the area covered with OTS SAMs. Such TiO_2 arrays on a SiO_2 background are a promising structure for biological applications as had been reported as a selective adhesion site in studying attachment of proteins or cells.[4,6,20] Second, nanocavity arrays in oxide films were also successfully formed using the PSCPs through a site-selective chemical etching (Figure 1e). For this process, PSCPs in OTS SAMs were made on an about 10-nm-thick,

(17) We estimated the attractive capillary force to be ∼210 MPa per a colloid in the case of a 350 nm particle, where one particle has seven interconnections (one particle−substrate and six particle−particle ones), using equations from Kralchevsky, P.; Nagayama, K. *Particles at Fluid Interfaces and Membranes*; Elsevier: Amsterdam, 2001; pp 469−502.

(18) Laarz, E.; Zhmud, B. V.; Bergström, L. *J. Am. Ceram. Soc.* **2000**, *83*, 2394.

(19) Wang, Y.; Lieberman, M. *Langmuir* **2003**, *19*, 1159.

(20) Michel, R.; Lussi, J. W.; Csucs, G.; Reviakine, I.; Danuser, G.; Ketterer, B.; Hubbell, J. A.; Textor, M.; Spencer, N. D. *Langmuir* **2002**, *18*, 3281.

thermally grown SiO_2 film supported by Si substrate underneath, and then the sample was immersed in buffered oxide etch (BOE) solutions.[21] Here the SAM layer of OTS functioned as a resistive layer during the etching, and only the opened areas of SiO_2 film dissolved, leaving the regular arrays of nanocavities. The SAM layer remains stable throughout this process as a result of the continuity of the layer formed by van der Waals forces that exist between carbon chains of OTS molecules. The average depth of the cavities was ~10 nm, and as etching time increases the enlargement of the cavities was observed as a result of "under cut" as in conventional wet etching. These freshly etched metal oxide holes and the surrounding OTS layers revealed superior patterns with high chemical contrasts.[22]

Upon the experimental affirmation that CAL successfully produces the desired patterns or features, we investigated the theoretical sizes of the holes in chemical patterns from a simple geometrical consideration of the contact area between the spherical particle and the substrate. Sizes of the individual holes in PSCPs with SAMs were calculated as follows:

$$d = \sqrt{\left(\frac{D}{2}\right)^2 - \left|t - \frac{D}{2}\right|^2} \qquad (1)$$

where d is the diameter of the resulting hole in the SAMs, D is the diameter of the spherical colloids (assuming an ideal solid sphere) used, and t is the thickness of the SAM layer. Typically, taking the thickness of OTS SAMs of 2.5 nm, we could expect hole diameters, d, to be 44, 59, and 71 nm when the silica colloids of 200, 350, and 500 nm in diameter are used, respectively. As the experimental results presented earlier, there were noticeable differences of about 10−20 nm between the calculated and the observed sizes. That is, the observed sizes were bigger than the calculated ones.

Differences between the two can be attributed to the liquid condensed in the meniscus between the colloids and the substrate. We believe that the liquid "capillary bridge", which was discussed above in relation to a strong structural integrity of the colloidal crystals, also plays a crucial role in determining the size of the resulting PSCPs in SAMs. We note that there are bridges of solid precipitates in addition to the liquid bridges. Considering their size in capillary compared with the liquid bridges, however, their contribution to the enlargement of the resulting holes can be ignored. We argue that the water molecules in the capillary could be a source for hydrolysis and polymerization of OTS molecules, enlarging the resulting sizes. In fact, the polymerized OTS molecules were often found around the holes when observed the patterns without a cleaning procedure after the removal step of colloids. We tried to remove the condensed liquid by replacing it with other solvents. Three different solvents were used in this study: a piranha solution, a 1:1 mixture

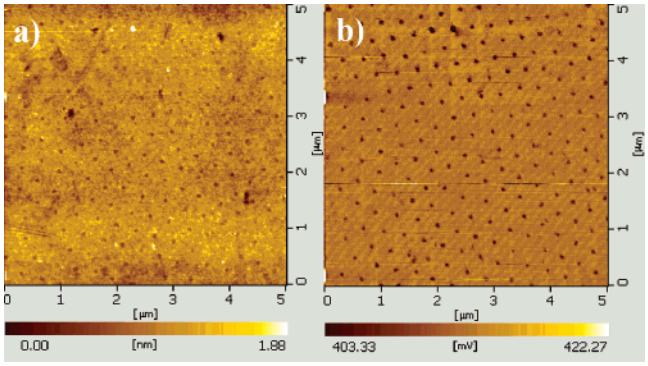

Figure 3. AFM topographical image (a) and the corresponding friction force image (b) of the chemical patterns in OTS−SAMs with the size of 60 ± 8 nm after acetone treatment, which is close to the expected value by the geometrical consideration when ~350 nm particles are used.

of water and ethanol, and acetone, which are in descending order in terms of their surface tension.[23] When the substrate was treated with the piranha solution, which has the highest tension among the three, the sizes of the resulting holes were 150−200 nm, much larger than those in our original experiments. It indicates that thicker capillary bridges were built up, causing the larger size of the patterns. In the case of the mixture of water and ethanol, which was the same solvent as the one used for dispersing the silica colloids, the same size as the case without solvent exchange was achieved (79 ± 7 nm). In comparison with the first two solvents, we achieved the pattern size of 60 ± 8 nm, which is very close to the calculated value (i.e., 59 nm) by using acetone. Acetone has a lower surface tension than the other two; thus, it successfully induced much thinner capillary liquid bridges yielding the smaller size of PSCPs. These results strongly support our argument that not only the geometry but also the liquid condensation contribute to the resulting hole sizes. Note that AFM could not resolve the topographical image of the PSCPs clearly when the substrate was treated with the liquid of lower surface tension such as acetone, although the friction force micrograph clearly reveals the distinct patterns as shown in Figure 3a,b. This is because washing the substrate with such liquid not only affects the resulting size of the PSCPs but also causes the incomplete growth of OTS SAMs, as it eliminates the water film on the hydrophilic oxide surfaces. In accordance with the growth mechanisms of OTS SAMs, OTS molecules need both hydroxyl groups in oxide surfaces and the water film of one or several molecular layers to grow into complete monolayer.[19] The lack of water molecules on the surface of the substrate, after washing it with acetone, prevents the complete growth of OTS molecules. The measured thickness of OTS SAMs, which was approximately 0.5 nm, indicates imperfect coverage or growth of the SAMs layer.[24] We acknowledge that there is a tradeoff between achievement of the PSCPs of calculated size with the use of solvent with lower surface energy and the complete growth of a SAM layer with the use of aqueous solutions. Thus, a modified equation that factors in the impact of capillary bridges and, hence, can

(21) BOE is known to provide a constant etch rate as a result of the presence of NH_4F and also suite organic resist because commercial hydrofluidic acid solution can penetrate the organic resist materials.

(22) We were not able to directly measure the contact angle with this pattern. We obtained the static contact angle of water in difference to be ~110° from two samples of a freshly etched SiO_2 film and a fully grown OTS−SAM layer independently.

(23) Surface tensions (mN m^{-1}, at 20 °C) of ingredients used in each solvent are as follows: H_2SO_4 (72−75), H_2O_2 (75), H_2O (72.8), C_2H_5OH (22.1), and CH_3COCH_3 (25.2).

(24) Schreiber, F. *Prog. Surf. Sci.* **2000**, *65*, 151.

correctly estimate an exact pattern size of PSCPs in SAMs when aqueous solutions are used is under study.

CAL has several significant improvements in fabricating nanometric chemical patterns. (1) CAL directly generates the chemical patterns without any additional surface modification processes. (2) It provides excellent isolation of the various inorganics resulting in nanostructures. In NSL, the defect structures of the colloidal films such as stacking faults and point defects as well as microcracks due to the shrinkage of the films in a vacuum chamber can result in the particles with overlapped feature. In contrast, the isolation of the features obtained from CAL is not influenced by the presence of these kinds of defects. (3) CAL can generate a smaller size of patterns than those created by traditional NSL when the colloids of the same size are used (with the exception of modified NSL techniques such as angle-resolved NSL).[25] The only exception to this is when particles smaller than ~100 nm are involved. However, note that the 2D close-packed arrays of the particles of such size are, in practice, very difficult to achieve without either using surfactant on the surface of the particles or using an apparatus that could lower thermal energy, *kT*, in a self-assembling system. (4) Finally, CAL does not require any vapor deposition equipment in fabricating the chemical patterns, as it is a chemical process. In conclusion, this strategy can be applied in creating a variety of combinations of surface chemical contrasts that can be served in biological applications, surface chemistry, and light harvesting structures.

The experimental details are as follows. OTS (95%, Aldrich), toluene (99.8%, anhydrous, Aldrich), ethanol (anhydrous, Carlo Erba), and acetone (99.5%, Aldrich) were commercially available and used as received. Deionized (DI) water, 15 MΩ cm milli-Q water, concentrated sulfuric acid (Duksan), H_2O_2 (38%, Duksan), and BOE (6:1, J. T. Baker) were used as obtained. Highly N-doped single side polished Si wafer of [100] orientation was cut into 1 × 1 cm pieces with a diamond glass cutter before cleaning.

Wafers were first cleaned with a Branson 1510 ultrasonic cleaner and sonicated in acetone and ethanol. The wafers were then rinsed with DI water and dried with a stream of N_2. The cleaned wafers were soaked in a 10:1 DI water/hydrofluidic acid solution for 1 min to remove the original native silicon oxide. After that, the wafers were blown dry with a stream of N_2. A piranha solution (70% v/v concentrated H_2SO_4, 30% v/v H_2O_2) was prepared in a clean beaker, and the wafers were soaked at 90 °C for 10 min to grow fresh native oxide. They were rinsed with DI water and blown dry with N_2.

Monodispersed silica particles, which were used as self-assembling building blocks in this study, were prepared by the Stöber process using tetraethoxyorthosilicate (TEOS, 99.9%, Aldrich), ethanol (99.9%, Aldrich), NH_4OH (28% NH_3 in water, Aldrich), and DI water as starting materials. TEOS was hydrolyzed by a small amount of water in ethanolic solutions with ammonia. The reagents were mixed and stirred in a water bath (Fisher isotemp heating circulator model no. 2013P) at 50 °C for 50−100 min, under a N_2 atmosphere. The sol was purified by several cycles of centrifugation, decantation, and resuspension in absolute ethanol to remove undesirable particles and to prevent continuous reaction, followed by drying in a vacuum oven at 100 °C. The particle populations used in this study had diameters of about 200, 350, and 500 nm. Measurement of the mean size and size distribution of the prepared SiO_2 colloidal particles was conducted by a light scattering system (Microtrac UPA-150).

OTS SAMs were grown by immersing the samples in anhydrous toluene solutions containing 0.1 vol % OTS for 5 h under ambient conditions. The wafers were rinsed with DI water to terminate the reaction of the active headgroup of the remaining OTS molecules. The assembled particles were detached through ultrasonication for 3 min in DI water. The OTS molecules physisorbed upon the OTS SAM layer were removed by sonicating the sample with DI water and pure toluene solution for 3 min, respectively. The surface of the sample was repeatedly rubbed with Q-tips smeared with toluene.

The ALD system of Cyclic 4000 (Genitech) was used to deposit TiO_2 onto the patterned hole of the OTS SAMs. The TiO_2 was deposited only onto the holes and not on the surfaces of the OTS SAMs at a temperature of 250 °C. Titanium iso-propoxide [$Ti(OCH(CH_3)_2)_4$] was used as the source of Ti. Water vapor with the flow rate of 5 sccm was used as an oxidant. N_2 was used as a carrier gas, and Ar gas was used for purging. The cycle consisted of 2 s of exposure to the Ti source, 5 s of Ar purge, 2 s of exposure to water, and 5 s of Ar purge. The total flow rate of the N_2 was 20 sccm. The thin films were grown under 2 Torr.

PSCPs in OTS SAMs, as-prepared TiO_2 nanodiscs, and SiO_2 nanocavities were imaged by contact-mode AFM (SPA-400, Seiko Instruments, Japan) using silicon nitride AFM tips with a small spring constant (SN-AF01, Olympus). Every average diameter and the size distribution were obtained by line-profiling the sizes of at least 100 features in the images, as determined by the full widths at half-maxima.

Acknowledgment. We thank Prof. Lennart Bergström (Stockholm University, Sweden) for helpful comments and suggestions. This work was supported by a grant (R01-2002-000-00318-0) from KOSEF. Both M.M.S. and J.M. independently thank the program of the National Research Laboratory of MOST. H.S. also thanks Center for Materials and Processes of Self-assembly (R11-2005-048-00000-0) by the ERC program of MOST/KOSEF.

CM052084M

(25) Haynes, C. L.; McFarland, A. D.; Smith, M. T.; Hulteen, J. C.; Van Duyne, R. P. *J. Phys. Chem. B* **2002**, *106*, 1898.